A Combined Experimental and Theoretical ^{17}O NMR Study of Crystalline Urea: An Example of Large Hydrogen-bonding Effects

Shuan Dong, Ramsey Ida, and Gang Wu*

Department of Chemistry, Queen's University, Kingston, Ontario, Canada K7L 3N6

Received: June 27, 2000

We report the first experimental determination of the carbonyl ^{17}O electric-field-gradient (EFG) tensor and chemical-shift (CS) tensor of a urea-type functional group, $R_1NH-C(O)-NHR_2$. Analysis of magic-angle spinning (MAS) and stationary ^{17}O NMR spectra of crystalline [^{17}O]urea yields not only the principal components of the carbonyl ^{17}O EFG and CS tensors, but also their relative orientations. The carbonyl ^{17}O quadrupole coupling constant (QCC) and the asymmetry parameter (η) in crystalline urea were found to be 7.24 ± 0.01 MHz and 0.92, respectively. The principal components of the ^{17}O CS tensor were determined: $\delta_{11} = 300 \pm 5$, $\delta_{22} = 280 \pm 5$ and $\delta_{33} = 20 \pm 5$ ppm. The direction with the least shielding, δ_{11}, is perpendicular to the C=O bond and the principal component corresponding to the largest shielding, δ_{33}, is perpendicular to the N−C(O)−N plane. The observed ^{17}O CS tensor suggests that, in crystalline urea, the ^{17}O paramagnetic shielding contributions from the $\sigma \rightarrow \pi^*$ and $\pi \rightarrow \sigma^*$ mixing are greater than that from the $n \rightarrow \pi^*$ mixing. Quantum chemical calculations revealed very large intermolecular H-bonding effects on the ^{17}O NMR tensors. It is demonstrated that inclusion of a complete intermolecular H-bonding network is necessary in order to obtain reliable ^{17}O EFG and CS tensors. B3LYP/D95** and B3LYP/6-311++G** calculations with a molecular cluster containing 7 urea molecules yielded ^{17}O NMR tensors in reasonably good agreement with the experimental data.

Introduction

Hydrogen bonding is a crucial element in the three-dimensional structures of biological systems such as proteins and nucleic acids.[1] Nuclear magnetic resonance (NMR) spectroscopy is among the most important and versatile techniques for studying hydrogen-bonding phenomena.[2−4] One of the most exciting recent developments involves direct observation of indirect spin−spin (*J*) coupling constants across a hydrogen bond in nucleic acids and proteins.[5−7] In recent years, solid-state NMR has also emerged as a useful technique in the study of hydrogen bonded systems.[8−12]

Among the elements that are often directly involved in a hydrogen bond, H, C, N and O, ^{17}O (spin = $^5/_2$ and natural abundance = 0.037%) NMR is far less common than NMR studies of ^1H, ^{13}C and ^{15}N nuclei. Although a considerable amount of literature on solution ^{17}O NMR has been accumulated over the past 50 years,[13−19] relatively little is known about the ^{17}O electric-field-gradient (EFG) *tensor* and chemical shielding (CS) *tensor* in organic and biological compounds. This is partly due to the experimental difficulties in measuring these second-rank tensors for quadrupolar ^{17}O nuclei. Nevertheless, the pioneering studies by Oldfield and co-workers[20−25] and by Ando and co-workers[26−28] have demonstrated the usefulness of solid-state ^{17}O NMR in the study of a variety of systems including biologically relevant molecules. Recently, we reported the experimental determination and quantum chemical calculation of ^{17}O EFG and CS tensors for a number of important functional groups.[29−31] However, to the best of our knowledge, no data are available in the literature concerning the carbonyl ^{17}O EFG and CS tensors in a urea-type functional group, $R_1NH-C(O)-NHR_2$. The urea-type carbonyl oxygen is common in nucleic acid bases such as thymine (T), uracil (U) and cytosine (C). Base pairing often involves a urea-type carbonyl oxygen atom, e.g., G:C and A:U base pairing. Therefore, it is of fundamental significance to characterize the ^{17}O EFG tensor and CS tensor for this type of functional group. We chose to study crystalline urea for several reasons. First, urea is the simplest form of the urea-type functional group ($R_1 = R_2 = H$) and is also one of the simplest biological molecules. Second, the crystal structure of urea has been accurately determined by both X-ray and neutron diffraction studies.[33−35] Third, crystalline urea exhibits unique hydrogen-bonding features, and is an ideal system for investigating the influence of hydrogen bonding on ^{17}O NMR tensors. The urea crystals form a tetragonal lattice with the space group $P\bar{4}2_1m$.[33−35] The urea molecule lies in a special position where the molecular point symmetry (*mm*2) is fully utilized. In the crystal lattice, the urea molecules are linked together by two hydrogen bonds in a "head-to-tail" fashion forming infinite ribbons along the crystallographic *c* axis. The neighboring ribbons are mutually orthogonal to one another; see Figure 1. Each oxygen atom of the urea molecule is directly involved in four C=O···H−N hydrogen bonds, two between the neighboring molecules in the same ribbon and the other two between the molecules from the two adjacent ribbons. This is the only example of a carbonyl oxygen atom which accepts four hydrogen bonds. Furthermore, since the urea molecule can serve both as a hydrogen bond donor (through N−H) and as an acceptor (through C=O), each urea molecule is directly hydrogen bonded to six surrounding urea molecules. Such unique hydrogen-bonding features of crystalline urea provide one with an ideal system for studying the influence of hydrogen bonding on ^{17}O EFG and CS tensors for a urea-type functional group. In this contribution, we report both experimental determination and quantum chemical calculations of the ^{17}O EFG tensor and CS tensor for crystalline [^{17}O]urea.

Experimental Section

Sample Preparation. Water (^{17}O 50.2% atom) was purchased from ISOTEC (Miamisburg, OH). Cyanamide (120 mg) and

* Corresponding author. Phone: 613-533-2644. Fax: 613-533-6669. E-mail: gangwu@chem.queensu.ca.

10.1021/jp002293o CCC: $19.00
Published on Web 11/02/2000

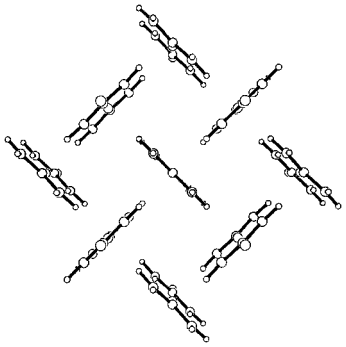

Figure 1. Crystal lattice of urea viewed along the *c* axis.

SCHEME 1

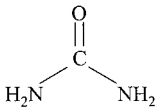

Urea

55 mg $H_2{}^{17}O$ were mixed and diluted with 0.6 mL anhydrous dioxane. After saturated with dry HCl at 0 °C, the solution was sealed and heated at 80 °C for 60 h (the reaction was traced by ^{17}O NMR). Upon removal of the solvent, the solids were dissolved in water. The [^{17}O]urea/HCl aqueous solution was obtained by filtering off the insoluble byproduct. A strong base resin, Amberite IRA-410, was used as a scavenger to remove the HCl in solution. Recrystallization from alcohol and ether yielded 105 mg of [^{17}O]urea (yield 67%). IR and solution NMR spectra were consistent with those reported in the literature.

Solid-State NMR. Solid-state ^{17}O NMR spectra were recorded on a Bruker Avance-500 spectrometer operating at 500.13 and 67.8 MHz for ^{1}H and ^{17}O nuclei, respectively. Polycrystalline [^{17}O]urea was packed into a zirconium oxide rotor (4 mm o.d.). The sample spinning frequency was 10 kHz. In the stationary ^{17}O NMR experiments, a Hahn-echo sequence was used to eliminate the acoustic ringing from the probe. A recycle delay of 60 s was used because of the long ^{17}O spin−lattice relaxation time in crystalline urea. A liquid sample of H_2O (25% ^{17}O atom) was used for RF power calibration as well as for ^{17}O chemical shift referencing, $\delta(H_2O,liq) = 0$ ppm. Spectral simulations were performed with the WSOLIDS program (Drs. Klaus Eichele and Rod Wasylishen, Dalhousie University).

Computational Aspects. All quantum chemical calculations on ^{17}O EFG and CS tensors were carried out with the Gaussian98 program[36] on a Pentium II personal computer (400 MHz, 128 MB RAM, 12 GB disk space). Standard basis sets such as STO-3G, 6-311G, D95**, 6-311G**, and 6-311++G** were used. Calculations were performed at both restricted Hartree−Fock (RHF) and density functional theory (DFT) levels. The B3LYP exchange functional[37] was employed in the DFT calculations. For chemical shielding calculations, the Gauge-Included Atomic Orbital (GIAO) approach[38] was used.

The principal components of the ^{17}O EFG tensor, q_{ii}, are computed in atomic units (a.u.). In solid-state NMR experiments, the observable quantity is the so-called quadrupole coupling tensor whose principal components are defined as $|\chi_{zz}| > |\chi_{yy}| > |\chi_{xx}|$. The two tensorial quantities are related by the following equation:

$$\chi_{ii}\,(\mathrm{MHz}) = e^2Qq_{ii}/h = -2.3496Q\,(\mathrm{fm}^2)\,q_{ii}\,(\mathrm{au}) \qquad (1)$$

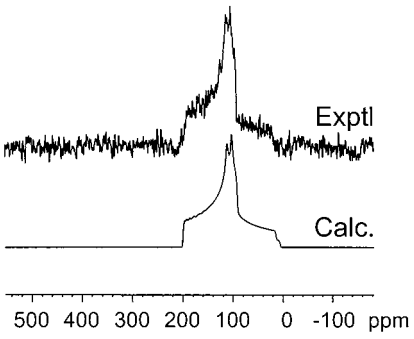

Figure 2. Calculated and experimental ^{17}O MAS spectra of crystalline [^{17}O]urea.

where Q is the nuclear quadrupole moment of the ^{17}O nucleus (in units of fm^2, 1 fm$^2 = 10^{-30}$ m^2) and the coefficient of 2.3496 arises from unit conversion.

In NMR experiments, the frequency of a NMR signal is determined relative to that arising from a standard sample. This relative quantity is known as the chemical shift, δ. In the case of ^{17}O NMR, the signal from a liquid H_2O sample is used as the chemical shift reference, $\delta(H_2O,liq) = 0$ ppm. Since quantum chemical calculations yield absolute chemical shielding values, σ, one must establish the absolute shielding scale for a particular nucleus in order to make direct comparison between calculated results and experimental data. For ^{17}O nuclei, an accurate absolute shielding scale was suggested by Wasylishen and co-workers.[39] We used the following equation to convert the calculated ^{17}O chemical shielding values to ^{17}O chemical shifts:

$$\delta = 307.9\ \mathrm{ppm} - \sigma \qquad (2)$$

where 307.9 ppm is the absolute chemical shielding constant for the ^{17}O nucleus in liquid H_2O.

Results and Discussion

^{17}O EFG and CS Tensors. Figure 2 shows the experimental and simulated ^{17}O MAS spectra of [^{17}O]urea. The observed ^{17}O MAS NMR spectrum exhibits a typical line shape arising from the second-order quadrupole interaction. Analysis of the ^{17}O MAS spectrum yielded that $\chi = e^2q_{zz}Q/h = 7.24 \pm 0.01$ MHz, $\eta = 0.92$, and $\delta_{iso} = 200 \pm 1$ ppm. The observed isotropic ^{17}O chemical shift in crystalline urea is consistent with that found in solution.[40] Interestingly, the urea carbonyl ^{17}O QCC is smaller than those observed for amide carbonyl oxygen nuclei.[31,32]

To determine the relative orientation between the ^{17}O EFG and CS tensors, we obtained a stationary ^{17}O NMR spectrum of urea; see Figure 3. Since the crystallographic symmetry of urea requires that the principal-axis-systems (PAS) of the carbonyl ^{17}O EFG and CS tensors are coincident, analysis of the stationary ^{17}O NMR spectrum becomes straightforward. In fact, there are only two possible relative orientations between the two NMR tensors: (A) $\alpha = 0$, $\beta = 90$, $\gamma = 90°$ and (B) $\alpha = 0$, $\beta = 90$, $\gamma = 0°$. In both cases, the direction with the largest shielding, δ_{33}, coincides the direction with the smallest EFG component, χ_{xx}. The only difference between the two possible situations is that δ_{11} is parallel to χ_{zz} and χ_{yy} for (A) and (B), respectively. Because of the fact that the ^{17}O EFG tensor exhibits $\eta = 0.92$ ($\chi_{zz} \approx \chi_{yy}$), the orientations (A) and (B) are actually very similar. Nevertheless, as shown in Figure 3, the orientation (B) clearly produces a better agreement with the experimental spectrum.

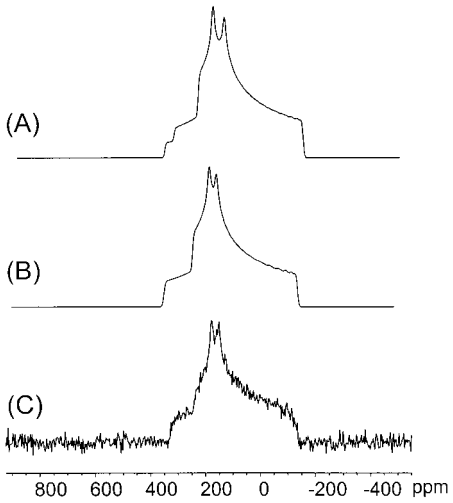

Figure 3. Calculated (A, B) and experimental (C) ^{17}O stationary NMR spectra of crystalline urea. In (A), $\alpha = 0$, $\beta = 90$, $\gamma = 90$ °. In (B), $\alpha = 0$, $\beta = 90$, $\gamma = 0$°. See text for discussion.

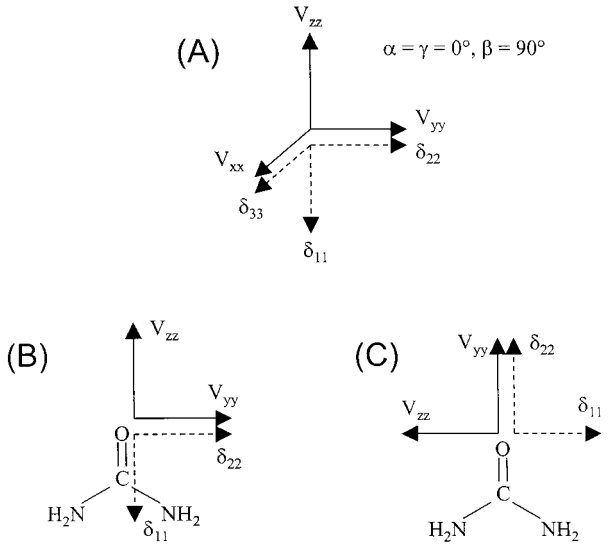

Figure 4. (A) Relative orientation between the ^{17}O EFG tensor and CS tensor as determined from analysis of the experimental stationary ^{17}O NMR spectrum. (B and C) Two possible absolute orientations of the ^{17}O EFG and CS tensors in the molecular frame. See text for discussion.

It is well-known that the aforementioned analysis of experimental NMR spectra yields only the *relative* orientation between EFG and CS tensors rather than the absolute tensor orientation in the molecular frame. Again, as a result of the crystallographic symmetry of crystalline urea, there are only two possible ways of placing the carbonyl ^{17}O EFG and CS tensors in the molecular frame, once the relative orientation between them is determined. The two possible situations are depicted in Figure 4. In the absence of any single-crystal ^{17}O NMR data, we decided to perform quantum chemical calculations in order to determine the absolute orientations of the ^{17}O EFG and CS tensors. Before we discuss the calculated results in detail, we will first describe the molecular models employed in the calculations.

Modeling the Hydrogen Bond Network in Crystalline Urea. As mentioned earlier, the presence of extensive intermolecular hydrogen bonding interactions in crystalline urea provides one with an ideal situation for examining the influence of these interactions on ^{17}O NMR tensors. To study systematically the hydrogen bonding effect in urea crystals, we constructed several molecular clusters with various sizes. As shown

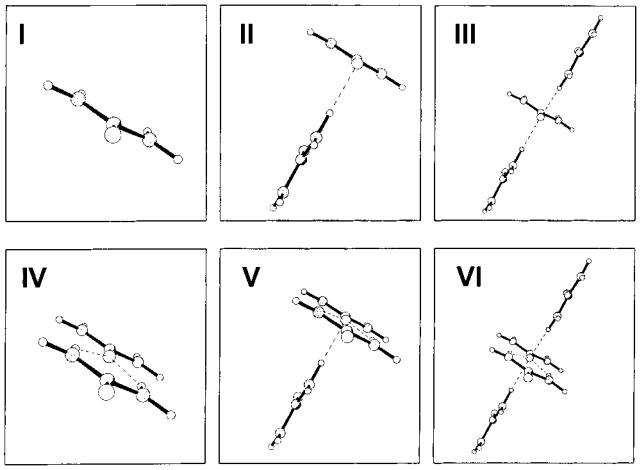

Figure 5. Urea molecular clusters (models I−VI).

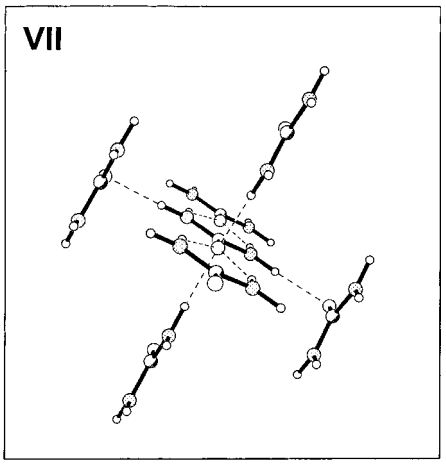

Figure 6. The largest urea molecular cluster used in the present study (model VII).

in Figures 5 and 6, a total of seven models were used in the quantum chemical calculations of this study. Model I consists of an isolated urea molecule with a planar C_{2v} geometry. This is different from the gas-phase structure of urea.[41−43] In addition, the C═O and C−N distances of the urea molecule in the solid state (1.265 and 1.349 Å)[33] are also quite different from the corresponding gas-phase values (1.221 and 1.378 Å).[42] For these reasons, the molecular geometry from a low-temperature (12 K) neutron diffraction study of crystalline urea[33] was directly used in the model construction without geometry optimization. Model II contains two urea molecules where the target molecule is hydrogen bonded to another urea molecule from the neighboring ribbon with an O···H distance of 1.992 Å. The two urea molecular planes are perpendicular to each other. Model III contains three molecules where the target molecule is also hydrogen-bonded to two molecules. However, the two urea molecules are from the two neighboring ribbons on both sides. The H-bond length is the same as in model II. In model IV, the two hydrogen bonded urea molecules are from the same ribbon, so they are planar forming a "head-to-tail" cyclic dimer with an O···H distance of 2.058 Å. It is interesting to note the difference between Models III and IV. In each model, the target oxygen atom forms two H-bonds. However, the urea molecules in model III form an H-bonded chain, whereas those in model IV are cyclic. As will be seen later, these structural differences have large effects on the ^{17}O NMR tensors. Model V consists of three urea molecules forming three H-bonds. Model VI is a tetramer where the target carbonyl oxygen atom is directly

TABLE 1: Experimental and Calculated (B3LYP) ^{17}O EFG Values for Small Molecules[a]

molecule	exp QCC (MHz)	calcd q_{zz} (au) STO-3G	6-311G	D95**	6-311G**	6-311++G**
CO[b]	4.337	0.0925	0.7264	0.4799	0.7264	0.6819
H_2CO[c]	12.35	2.3118	2.2417	2.1909	2.2417	2.1648
H_2O[d]	10.1068	2.6956	2.0398	1.8586	2.0398	1.8070
MeOH[e]	11	2.5545	2.0872	1.9424	2.0872	1.9321
SCO[f]	−1.32	−0.7334	−0.2678	−0.4080	−0.2678	−0.2735
SO_2[g]	6.6	1.9449	1.3130	1.3274	1.3130	1.3077

[a] All calculations were based on the microwave structures. [b] From ref 49. [c] From ref 50. [d] From ref 51. [e] From ref 52. [f] From ref 53. [g] From ref 54.

involved in four C═O···H—N hydrogen bonds, two from the neighboring molecule in the same ribbon and the other two from adjacent ribbons. This model is a reasonably good description of the H-bonding network in crystalline urea.

As illustrated in Figure 6, model VII is the largest molecular cluster employed in the present study. In this model, the target molecule serves both as an H-bond acceptor and as a donor resulting in additional H-bonds. In particular, the target molecule is at the center of a ribbon fragment containing three urea molecules to which four additional molecules from four different neighboring ribbons are hydrogen bonded. Consequently, model VII represents a complete quantitative description of the H-bond network around the target urea molecule in crystal lattice. It is worth noting that, although model VII contains a total of 56 atoms, the high crystallographic symmetry of the cluster has considerably reduced the demand for computing power. For example, a total of 812 basis functions (1260 primitive Gaussians) were used in the B3LYP/6-311++G** calculations for model VII. The EFG and GIAO-shielding calculations took approximately 9 h and 5 days, respectively. As will be shown in the following sections, model VII is able to produce quite satisfactory results for the ^{17}O NMR tensors.

Calculations of the ^{17}O EFG Tensor. In this section, we will focus on the quantum chemical ^{17}O EFG calculations for crystalline urea. To make direct comparison between the calculated EFG tensor and the observed quadrupole coupling tensor, it is necessary to know the ^{17}O nuclear quadrupole moment, Q; see eq 1. Since large variations (up to 30%) exist in the literature concerning the value of $Q(^{17}O)$, it is difficult to compare directly the calculated EFG results with the observed QCC value. Recently, several groups demonstrated a calibration approach, based on which an effective ^{17}O quadrupole moment can be derived for a particular level of theory.[44−47] The calibration procedure consists of three steps. First, one selects a group of small molecules for which accurate values of ^{17}O QCCs have been determined by high-resolution microwave spectroscopy. Second, one calculates the EFG values for these small molecules at a particular level of theory. Finally, one adjusts the value of Q to minimize the errors between the calculated QCC values and the observed data using eq 1. Following this procedure, we calculated the ^{17}O EFGs for several small molecules at both RHF and DFT levels with various basis sets. The DFT results are presented in Table 1 (the RHF results are not shown). Combining the calculated EFGs and the experimental QCC values, we obtained the effective Q values at different levels of theory. The calibrated Q values are summarized in Table 2 and a typical calibration plot is shown in Figure 7. As seen from Figure 7, the B3LYP/6-311++G** calculations yield reliable ^{17}O EFG results (<0.4 MHz) when an effective Q of −2.3935 fm^2 is used. This calibrated Q value is consistent with those calibrated at similar levels of accuracy.[44−47] It should be noted that all effective $Q(^{17}O)$ values shown in Table 2 are smaller than the standard value of −2.558 fm^2 recommended by Pyykko,[48] indicating that all approximation methods tend to overestimate ^{17}O EFGs.

TABLE 2: Calibrated $Q(^{17}O)$ Values at RHF and DFT Levels with Various Basis Sets

method	basis set	calibrated Q/fm^2	R^2	std error/MHz
RHF	STO-3G	−1.8508	0.8317	2.716
	6-311G	−1.9603	0.9103	1.666
	D95**	−2.2366	0.9498	1.297
	6-311G**	−2.1822	0.9840	0.6623
	6-311++G**	−2.2851	0.9775	0.788
B3LYP	STO-3G	−1.9080	0.8473	2.522
	6-311G	−2.0365	0.9475	1.230
	D95**	−2.3816	0.9720	0.944
	6-311G**	−2.2436	0.9920	0.463
	6-311++G**	−2.3935	0.9932	0.429

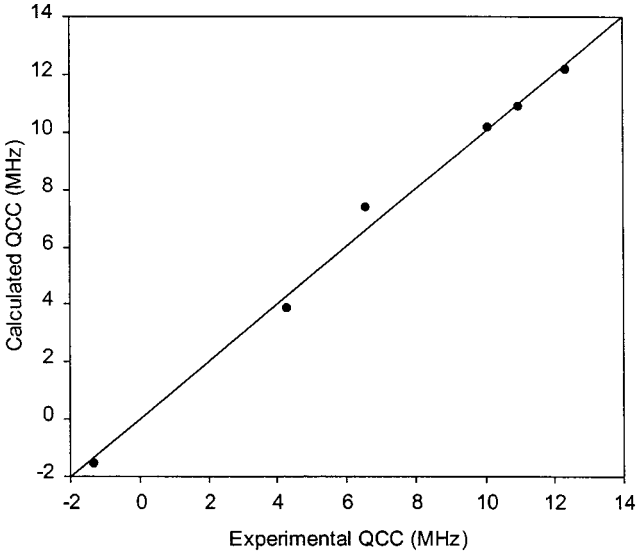

Figure 7. Comparison between the experimental and calculated (B3LYP/6-311++G**) ^{17}O QCCs for CO, H_2CO, H_2O, MeOH, SCO and SO_2. See Table 1 for data.

The effectiveness of the aforementioned calibration approach for crystalline urea is illustrated in Figure 8 where the basis set dependence of ^{17}O QCCs is shown. Clearly, if the standard Q value (−2.558 fm^2) is used, the calculated EFGs converge slowly as the size of the basis set is increased. However, even at the B3LYP/6-311++G** level, the calculated ^{17}O QCC for crystalline urea is approximately 1 MHz larger than the observed value, 7.24 MHz. In contrast, if the calibrated Q values are used, all calculations produce dramatically improved results. Under such circumstance, the discrepancy between the calculated and observed QCCs is less than 0.4 MHz, except for those with the minimal basis set STO-3G. Our observation strongly suggests that the calibration approach can be safely extended to molecular systems containing extensive H-bonding interactions.

The ^{17}O EFG calculations also confirmed that the carbonyl ^{17}O EFG tensor orientation is in agreement with the one depicted in Figure 4C. This ^{17}O EFG tensor orientation is also similar to that found for amide carbonyl groups.[31,32] However, it is interesting to note that the asymmetry parameter is close to 1 for the urea-type carbonyl oxygen whereas this parameter is always less than 0.5 in amides.[31,32]

Calculations of the ^{17}O Chemical Shielding Tensor. Unlike EFG calculations, quantum chemical calculations yield absolute shielding tensors that can be directly compared with the experimental data using eq 2. However, it is still important to evaluate the basis set dependence. Extensive theoretical work has been done in this area; however, most previous studies have mainly focused on the isotropic ^{17}O chemical shielding constants

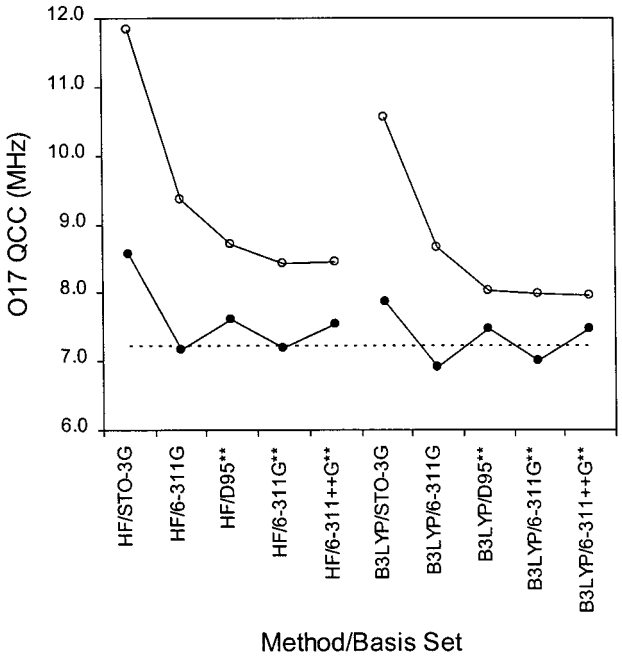

Figure 8. Basis set dependence of the calculated ^{17}O QCCs for crystalline urea. Model IV was used in the calculations. Open circles represent the results using the standard Q value of -2.558 fm^2, whereas the filled circles are obtained with the effective Q values shown in Table 2. The dash line indicates the experimental value.

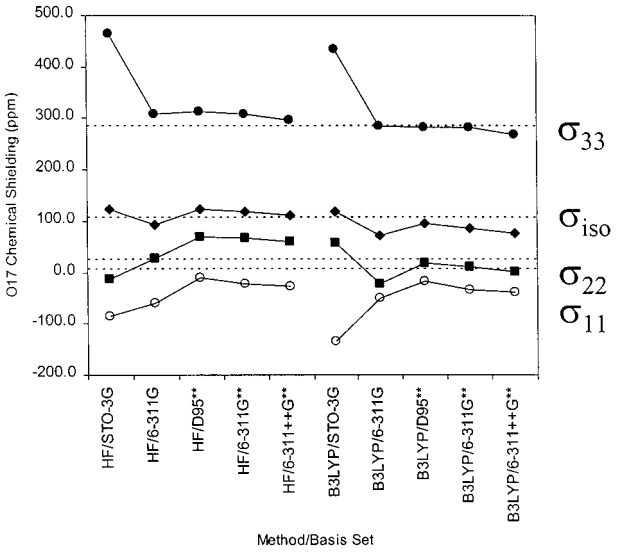

Figure 9. Basis set dependence of the calculated ^{17}O CS tensor. Model IV was used in the calculations. The dash lines indicate the experimental values.

arising from a handful of isolated small molecules.[55−64] It remains an open question as to whether extensive hydrogen-bonded molecular clusters present some new challenges to the current quantum chemical methodologies. In several recent studies, we examined the ^{17}O CS tensors of various oxygen-containing functional groups in extensive H-bonding environment.[29−32] These studies suggested that B3LYP/D95** and B3LYP/6-311++G** calculations are adequate in reproducing experimental ^{17}O NMR results. In the present study, since we have already determined experimentally the ^{17}O CS tensor for crystalline urea, it is desirable to further test the basis set dependence for the ^{17}O shielding calculations in systems with very extensive hydrogen bonding. The calculated ^{17}O shielding results with model VI are shown in Figure 9. One general trend in Figure 9 is that the B3LYP calculations produce results similar to those of RHF. Another trend is that the polarization functions appear to be necessary to generate results in better agreement with the experimental data. Except for STO-3G, all basis sets can reproduce reasonably well the tensor component with the largest shielding, σ_{33} (or δ_{33}). Meanwhile other two principal components, σ_{11} and σ_{22} (or δ_{11} and δ_{22}), are within approximately 50 ppm to the experimental values. As will be shown later, this disagreement arises largely from the fact that model VI is an incomplete description of the H-bonding environment in crystalline urea.

Hydrogen Bonding Effects in Crystalline Urea. In this section, we will examine the H-bonding effects in the quantum chemical calculations of ^{17}O EFG and CS tensors. The calculated results from Models I through VII are summarized in Table 3. Using $Q = -2.3935$ fm^2, which is calibrated for B3LYP/6-311++G**, the calculated ^{17}O quadrupole coupling tensors for the urea clusters are shown in Figure 10A. Considering that the standard deviation arising from the Q calibration procedure is approximately ± 0.5 MHz, the agreement between the calculated and experimental data is excellent for Models VI and VII. In general, as the number of H-bonds is increased, the ^{17}O QCC decreases. More specifically, the ^{17}O QCC is decreased by approximately 1 MHz from an isolated urea molecule (model I) to a 7-molecule cluster (model VII). This is in agreement with the general trend observed in previous ^{17}O NQR studies.[65,66] Another interesting trend seen from Figure 10A is that χ_{zz} and χ_{xx} exhibit larger changes than χ_{yy}. This is also reflected in the changes of the asymmetry parameter, η. For example, η is increased from 0.66 in model I to 0.93 in model VII. We have recently observed a similar trend for the ^{17}O quadrupole coupling tensors in amides.[31, 32]

The calculated ^{17}O chemical shielding tensor components for various models are shown in Figure 10B. The principal components of the ^{17}O CS tensor are quite sensitive to the H-bond strength. Interestingly the three CS tensor components also exhibit different dependencies. The principal component with the largest shielding, δ_{33}, shows a decrease of approximately 40 ppm from Models I to VII, whereas the other two components, δ_{11} and δ_{22}, exhibit increases of more than 120 ppm. Consequently the span of the chemical shift anisotropy ($\delta_{11} - \delta_{33}$) is decreased from Models I through VII by approximately 170 ppm! For an isolated urea molecule, the calculated isotropic ^{17}O chemical shielding constant is smaller than the experimental value by 80 ppm. When the four direct H-bonds are considered in model VI, the deviation between the calculated and observed isotropic ^{17}O chemical shielding is reduced to 30 ppm. With model VII, the isotropic ^{17}O chemical shielding constant is in excellent agreement with the observed value (the discrepancy is less than 2 ppm). However, as we have emphasized previously,[30] examination of the calculated isotropic chemical shielding constant alone can be misleading. In fact, as clearly seen from Figure 10B, the calculated tensor components show deviations as large as 20 ppm from the experimental values. The apparent agreement between the calculated and observed isotropic shielding constants simply arises from the mutual cancellation of errors in the tensor components.

At first glance, it is somewhat surprising to see that, although model VI yields quite satisfactory ^{17}O quadrupole tensor results, the calculated ^{17}O chemical shielding tensor from this model shows a discrepancy of approximately 50 ppm in the δ_{11} component. The significant improvement of model VII over model VI in the calculations of the ^{17}O chemical shielding tensor is also surprising. Our results suggest that the neighboring urea molecules not directly involved in the H-bonding to the target oxygen nucleus can make a contribution of as large as 40 ppm

TABLE 3: Experimental and Calculated (B3LYP/6-311++G) Carbonyl ^{17}O Chemical Shielding Tensors and Quadrupole Coupling Tensors for Crystalline Urea**

model	σ_{iso}/ppm	σ_{11}/ppm	σ_{22}/ppm	σ_{33}/ppm	χ_{zz}/MHz	χ_{yy}/MHz	χ_{xx}/MHz
I	28.8	−114.8	−97.4	298.7	8.324	−6.918	−1.405
II	44.4	−85.6	−71.4	290.4	8.189	−7.069	−1.120
III	62.8	−59.2	−21.4	268.9	8.064	−7.182	−0.882
IV	46.0	−83.4	−47.9	269.2	7.731	−7.135	−0.596
V	62.7	−62.9	−41.9	292.9	7.590	−7.236	−0.355
VI	77.2	−38.8	1.7	268.8	7.459	−7.318	−0.142
VII	106.7	9.4	49.4	261.3	7.312	−7.049	−0.264
exp[a]	108 ± 1	8 ± 5	28 ± 5	288 ± 5	7.24 ± 0.01	−6.95 ± 0.01	−0.29 ± 0.01

[a] Experimental chemical shift tensor components are converted to the shielding scale using eq 2.

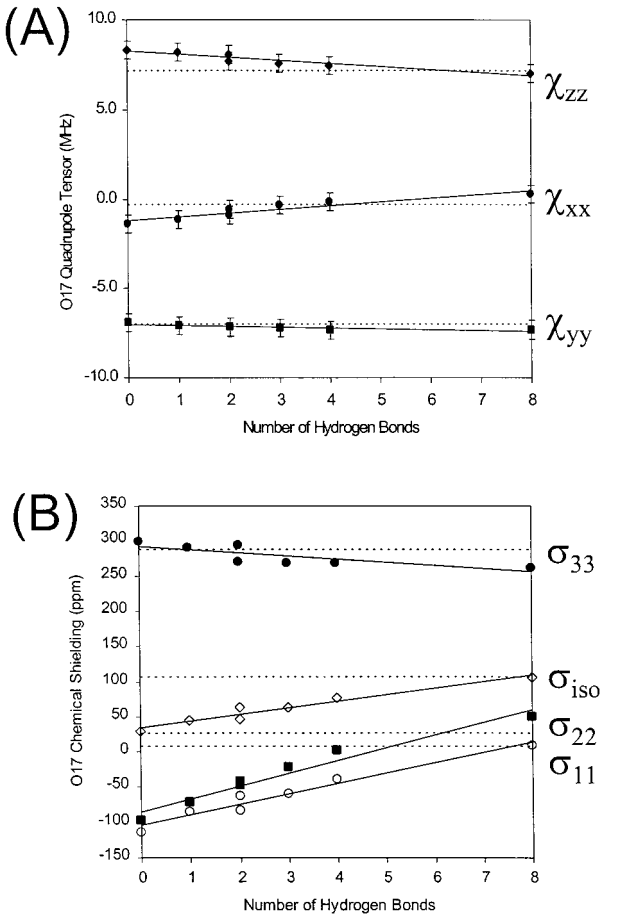

Figure 10. (A) Calculated (B3LYP/6-311++G**) ^{17}O quadrupole coupling tensors for models I-VII. The error bars indicate the uncertainty arising from the *Q* calibration. (B) Calculated (B3LYP/6-311++G**) ^{17}O chemical shielding tensors for models I-VII. The dash lines in both (A) and (B) indicate the experimental values.

to the ^{17}O chemical shielding tensor component. Clearly such a long-range ^{17}O shielding effect is transmitted via four chemical bonds, i.e., O═C−N−H···O. Similar long-range effects arising from intermolecular H-bonds have been observed previously in the ^{13}C shielding calculations of α-glycine.[67] The remaining small disagreement between the calculated results from model VII and experimental data may arise largely from the intrinsic limitation of the B3LYP/6-311++G** approach.

At this point, it is of interest to compare the ^{17}O EFG and CS tensors determined for urea with our previous results for a structurally related primary amide, benzamide.[31] The basic structural parameters for the amide fragment of benzamide[68] are *r*(C═O) 1.245 Å, *r*(C−N) 1.340 Å and ∠(O−C−N) 122.3°. The corresponding values for the urea molecule in the solid state are *r*(C═O) 1.265 Å, *r*(C−N) 1.349 Å and ∠(O−C−N) 121.4°. It is noted that the urea C═O bond length is considerably longer than that of benzamide. In contrast, the C−N bond

SCHEME 2

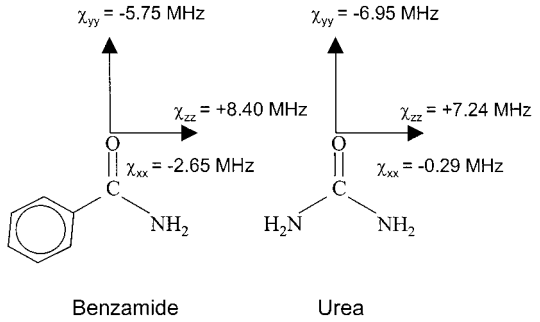

lengths in the two compounds are essentially the same. It should be pointed out that these solid-state structural parameters are quite different from those of the optimized molecular structures.[69] It is important to select the relevant molecular geometry when carrying out quantum chemical calculations for NMR tensors and comparing the calculated results with solid-state NMR data. In the crystal lattice, benzamide molecules form cyclic dimers linked laterally to form ribbons along the *b* axis,[68] where each oxygen atom is involved in two H-bonds. The ^{17}O QCC in benzamide, 8.40 MHz, is considerably larger than that in urea, 7.24 MHz. The asymmetry parameters of the two ^{17}O quadrupole tensors are also different, i.e., $\eta = 0.37$ for benzamide and $\eta = 0.92$ for urea. In fact, we found that the carbonyl oxygen nuclei in amides usually exhibit $\eta < 0.5$ whereas the urea-type oxygen nuclei have $\eta \approx 1$. It is noted however that the orientations of the ^{17}O quadrupole coupling tensor are the same for the two compounds. Our observation is in excellent agreement with the early ^{17}O NQR results reported by Cheng and Brown for a variety of organic carbonyl compounds.[70] On the basis of the simple Towns-Dailey analysis of Cheng and Brown, the simultaneous decrease in ^{17}O QCC and increase in η observed for urea indicate a lowered π bond order between the carbon and oxygen atoms with consequent increase in π orbital population. The large ^{17}O chemical shift difference (approximately 100 ppm) between the amide oxygen and urea oxygen nuclei is well-known and has been related to the difference in the $n \rightarrow \pi^*$ energy gap for these two classes of carbonyl compounds.[40] According to Ramsey's theory,[71] the nuclear magnetic shielding for molecules can be expressed as the sum of diamagnetic and paramagnetic contributions:

$$\sigma = \sigma_{ii}^{d} + \sigma_{ii}^{p} \tag{3}$$

where the subscript ii indicates the individual principal components of the shielding tensor ($i = x, y, z$). For $i = x$, the two shielding contributions can be written as[71]

$$\sigma_{xx}^{d} = \frac{\mu_0}{4\pi}\frac{e^2}{2mc^2}\left\langle 0\left|\sum_j \frac{(y_j^2 + z_j^2)}{r_j^3}\right|0\right\rangle \tag{4}$$

SCHEME 3

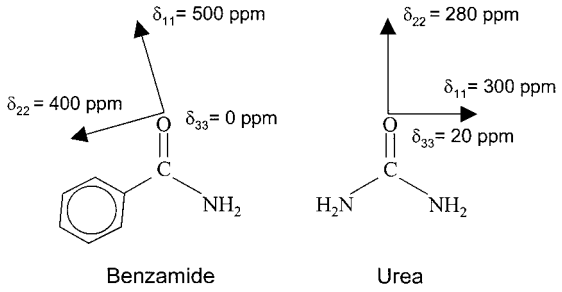

where ⟨0| is the ground-state electronic wave function, the sum

$$\sigma_{xx}^{p} = \frac{\mu_0}{4\pi}\frac{e^2}{2mc^2}\sum_{k>0}\left[\frac{\langle 0|\sum_j L_{xj} r_j^{-3}|k\rangle\langle k|\sum_j L_{xj}|0\rangle + cc}{E_0 - E_k}\right] \quad (5)$$

over k is over all excited electronic states, the sum over j is over all electrons, L_x is the electron orbital angular momentum operator, r_j is the distance between the jth electron and the nucleus of interest, cc indicates complex conjugate, E_0 and E_k are the energy values for the ground- and excited-states, respectively, other symbols such as μ_0, e, m and c are standard constants. Qualitatively, the diamagnetic shielding term is dominated by the core electrons and consequently exhibits little orientation dependence. On the other hand, the paramagnetic shielding contribution is responsible for the anisotropic nature of the shielding tensor. It is clear from eq 5 that the paramagnetic shielding term is inversely proportional to the energy gap between the ground state and the excited state. For carbonyl compounds, the HOMO−LUMO n → π^* transition often exhibits much smaller energy than other transitions, thereby becoming the predominant factor in the paramagnetic shielding at the oxygen nucleus. For this reason, current understanding of the ^{17}O chemical shielding trend in carbonyl compounds is based sorely on energy consideration. For example, the n → π^* energy separation in benzamdie is estimated to be 4.62 eV, based on the UV data (λ_{max} = 268 nm).[72] The corresponding energy gap in urea is much larger, ca. 6.75−7.14 eV.[73,74] The large n → π^* transition energy in urea can be attributed to the presence of two strong π-donating NH_2 groups, which leads to a destabilization of both the π^* and the n MOs. Therefore, it seems reasonable that urea exhibits a greater ^{17}O chemical shielding (or a smaller chemical shift value) than benzamide.

However, often neglected in previous studies of ^{17}O chemical shielding is the term involving the electron orbital angular momentum operator, $\mathbf{L} = (L_x, L_y, L_z)$, in eq 5. The detailed effects of the orbital angular momentum operator have been described by Jameson and Gutowsky.[75] Essentially, this term determines the direction along which the paramagnetic shielding contribution arising from a particular mixing between the ground state and an excited state is operative. For example, an n → π^* mixing contributes only to the shielding along the C═O bond, whereas a $\sigma \rightarrow \pi^*$ or $\pi \rightarrow \sigma^*$ mixing is responsible only for the paramagnetic shielding along the direction perpendicular to the C═O bond. Consequently, any information about the directions of the CS tensor components may shed more light on the origin of the observed shielding. In this regard, it is more informative to examine the entire shielding tensor rather than the isotropic shielding constant alone.

The orientation of the oxygen CS tensor within the carbonyl fragment has been thought to be invariant. An early theoretical work by Gierke and Flygare[76] indicated that for formaldehyde the ^{17}O CS tensor component with the largest paramagnetic shielding, δ_{11}, lies along the C═O bond. A later single-crystal NMR study confirmed that δ_{11} is parallel to the C═O bond in benzophenone.[77] Recently we found that this is also the case in both primary and secondary amides.[29,31,32] All these findings support the rationalization that the paramagnetic shielding contribution from the n → π^* mixing is predominant in carbonyl compounds. Intuitively, one would expect that the orientation of the ^{17}O CS tensor in urea would be similar to that in benzamide. Apparently, this is not the case. As mentioned earlier, the δ_{11} component of the ^{17}O CS tensor is perpendicular to the C═O bond of the urea molecule! This immediately suggests that the paramagnetic contributions arising from $\sigma \rightarrow \pi^*$ and $\pi \rightarrow \sigma^*$ mixing become larger than that from the n → π^* mixing. This appears to be the first example where the ^{17}O shielding in a carbonyl compound is not dominated by the n → π^* mixing. A recent LORG calculation of the carbonyl ^{17}O shielding in amides[78] suggests that the shielding contribution from the oxygen nonbonding orbital n_O is larger than that from σ(C═O) by approximately 50%. It may not be that surprising then that the order of these contributions is reversed in the case of urea. It is also worth noting that, for an isolated urea molecule (model I), the ^{17}O CS tensor is essentially axially symmetric. This indicates that isolated urea molecule is the critical point at which the relative magnitude of the paramagnetic shielding contributions from $\sigma \rightarrow \pi^*$ and $\pi \rightarrow \sigma^*$ mixing and from the n → π^* mixing begins to switch. Therefore, one should relate the shielding change along the C═O bond to the difference in the n → π^* gaps. In the case of benzamide and urea, this represents a change of 220 ppm. Meanwhile the shielding change along the direction perpendicular to the C═O bond is much smaller, ca. 100 ppm, suggesting that the $\sigma \rightarrow \pi^*$ and $\pi \rightarrow \sigma^*$ energy gaps are similar in the two compounds.

Conclusions

We have reported the first experimental determination of the carbonyl ^{17}O EFG tensor and CS tensor for crystalline urea. The extensive H-bonding in crystalline urea provides us with an ideal model for studying the dependence of ^{17}O NMR tensors on H-bonding environment. The quantum chemical calculations revealed that the presence of the four direct C═O···H—N hydrogen bonds in crystalline urea causes a decrease of 1 MHz in the carbonyl ^{17}O QCC and an increase of 50 ppm in the isotropic ^{17}O chemical shielding constant. In addition, the long-range effects due to the indirect H-bonds could contribute as large as 40 ppm to the ^{17}O CS tensor components. Consequently, it is important to include a complete H-bonding network in quantum chemical calculations in order to produce reliable ^{17}O NMR tensors.

The new finding of the present investigation suggests that, for the urea-type functional group, the paramagnetic shielding contributions arising from the $\sigma \rightarrow \pi^*$ and $\pi \rightarrow \sigma^*$ mixing are larger than that from the n → π^* mixing. This is a unique feature of the ^{17}O CS tensor for the urea carbonyl oxygen nucleus. The present study illustrates the importance of examining the entire CS tensor rather than the isotropic shielding constant alone. Calculations at both B3LYP/D95** and B3LYP/6-311++G** levels can reproduce reasonably well the experimental results provided that a complete H-bond network is included. The ^{17}O EFG and CS tensors determined for crystalline urea can be used as benchmark values for similar functional groups in nucleic

acid bases. Solid-state ^{17}O NMR may be useful in probing base pairing in nucleic acids.

Acknowledgment. We wish to thank the Natural Sciences Engineering Research Council (NSERC) of Canada for research and equipment grants. This research was partially supported by a grant from the Advisory Research Committee of Queen's University. G. W. also thanks Queen's University for a Chancellor's Research Award (2000-2005) and the Ontario government for a Premier's Research Excellence Award (2000-2005).

References and Notes

(1) Jeffrey, G. A.; Saenger, W. *Hydrogen Bonding in Biological Structures*; Springer-Verlag: Berlin, 1991.

(2) Ernst, R. R.; Bodenhausen, G.; Wokaun, A. *Principles of Nuclear Magnetic Resonance in One and Two Dimensions*; Clarendon Press: Oxford, 1987.

(3) Wüthrich, K. *NMR of Proteins and Nucleic Acids*; John Wiley & Sons: New York, 1986.

(4) Evans, J. N. S. *Biomolecular NMR Spectroscopy*; Oxford University Press Inc.: New York, 1995.

(5) Dingley, A. J.; Grzesiek, S. *J. Am. Chem. Soc*. **1998**, *120*, 8293.

(6) Pervushin, K.; Ono, A.; Fernandez, C.; Szyperski, T.; Kainosho, M.; Wüthrich, K. *Proc. Natl. Acad. Sci. U.S.A.* **1998**, *95*, 14147.

(7) Cordier, F.; Grzesiek, S. *J. Am. Chem. Soc*. **1999**, *121*, 1601.

(8) Asakawa, N.; Kameda, T.; Kuroki, S.; Kurosu, H.; Ando, S.; Ando, I.; Shoji, A. *Annu. Rep. NMR Spectrosc.* **1998**, *35*, 55.

(9) Brunner, E.; Sternberg, U. *Prog. Nucl. Magn. Reson. Spectrosc*. **1998**, *32*, 21.

(10) (a) Anderson-Altman, K. L.; Phung, C. G.; Mavromoustakos, S.; Zhang, Z.; Facelli, J. C.; Poulter, C. D.; Grant, D. M. *J. Phys. Chem*. **1995**, *99*, 10454. (b) Facelli, J. C.; Pugmire, R. J.; Grant, D. M. *J. Am. Chem. Soc*. **1996**, *118*, 5488. (c) Facelli, J. C. *Chem. Phys. Lett*. **2000**, *322*, 91.

(11) (a) Gu, Z.; McDermott, A. E. *J. Am. Chem. Soc*. **1993**, *115*, 4282. (b) Gu, Z.; Zambrano, R.; McDermott, A. E. *J. Am. Chem. Soc*. **1994**, *116*, 6368. (c) Gu, Z.; Ridenour, C. F.; McDermott, A. E. *J. Am. Chem. Soc*. **1996**, *118*, 822. (d) Wei, Y.; de Dios, A. C.; McDermott, A. E. *J. Am. Chem. Soc*. **1999**, *121*, 10389.

(12) Wu, G.; Freure, C. J.; Verdurand, E. *J. Am. Chem. Soc*. **1998**, *120*, 13187.

(13) Klemperer, W. G. *Angew. Chem., Int. Ed. Engl.* **1978**, *17*, 246.

(14) Kintzinger, J. P. In *NMR Basic Principles and Progress*, Diehl, P.; Fluck, E.; Kosfeld, R. Eds.; Springer-Verlag: Berlin, 1981; Vol. 17, pp 1−65.

(15) Fiat, D. *Bull. Magn. Reson.* **1984**, *4*, 30.

(16) McFarlane, W.; McFarlane, H. C. E. In *Multinuclear NMR*; Mason, J., Ed.; Plenum Press: New York, 1987; Chapter 14, pp 403−416.

(17) *17.Oxygen-17 NMR Spectroscopy in Organic Chemistry*; Boykin, D. W., Ed.; CRC Press: Boca Raton, FL, 1991.

(18) Gerothanassis, I. P. In *Encyclopedia of Nuclear Magnetic Resonance*, Grant, D. M., Harris, R. K., Eds.; John Wiley and Sons: New York, 1996; pp 3430−3440.

(19) Pearson, J. G.; Oldfield, E. In *Encyclopedia of Nuclear Magnetic Resonance*; Grant, D. M., Harris, R. K., Eds.; John Wiley and Sons: New York, 1996; pp 3440−3443.

(20) Schramm, S.; Kirkpatrick, R. J.; Oldfield, E. *J. Am. Chem. Soc*. **1983**, *105*, 2483.

(21) Schramm, S.; Oldfield, E. *J. Am. Chem. Soc.* **1984**, *106*, 2502.

(22) Walter, T. H.; Turner, G. L.; Oldfield, E. *J. Magn. Reson.* **1988**, *76*, 106.

(23) Salzmann, R.; Kaupp, M.; McMahon, M. T.; Oldfield, E. *J. Am. Chem. Soc*. **1998**, *120*, 4771.

(24) McMahon, M. T.; deDios, A. C.; Godbout, N.; Salzmann, R.; Laws, D. D.; Le, H.; Havlin, R. H.; Oldfield, E. *J. Am. Chem. Soc*. **1998**, *120*, 4784.

(25) Godbout, N.; Sanders, L. K.; Salmann, R.; Havlin, R. H.; Wojdelski, M.; Oldfield, E. *J. Am. Chem. Soc*. **1999**, *121*, 3829.

(26) Kuroki, S.; Takahashi, A.; Ando, I.; Shoji, A.; Ozaki, T. *J. Mol. Struct*. **1994**, *323*, 197.

(27) Kuroki, S.; Ando, S.; Ando, I. *Chem. Phys*. **1995**, *195*, 107.

(28) Yamauchi, K.; Kuroki, S.; Ando, I.; Ozaki, T.; Shoji, A. *Chem. Phys. Lett*. **1999**, *302*, 331.

(29) Dong, S.; Yamada, K.; Wu, G. *Z. Naturforsch.* **2000**, *55A*, 21.

(30) Wu, G.; Hook, A.; Dong, S.; Yamada, K. *J. Phys. Chem. A* **2000**, *104*, 4102.

(31) Wu, G.; Yamada, K.; Dong, S.; Grondey, H. *J. Am. Chem. Soc*. **2000**, *122*, 4215.

(32) Yamada, K.; Dong, S.; Wu, G. *J. Am. Chem. Soc*., submitted for publication.

(33) Swaminathan, S.; Craven, B. M.; McMullan, R. K. *Acta Crystallogr*. **1984**, *B40*, 300.

(34) Pryor, A.; Sanger, P. L. *Acta Crystallogr*. **1970**, *A26*, 543.

(35) Guth, H.; Heger, G.; Klein, S.; Treutmann, W.; Scheringer, C. *Z. Kristallogr*. **1980**, *153*, 237.

(36) Frisch, M. J.; Trucks, G. W.; Schlegel, H. B.; Scuseria, G. E.; Robb, M. A.; Cheeseman, J. R.; Zakrzewski, V. G.; Montgomery, J. A.; Stratmann, R. E.; Burant, J. C.; Dapprich, S.; Millam, J. M.; Daniels, A. D.; Kudin, K. N.; Strain, M. C.; Farkas, O.; Tomasi, J.; Barone, V.; Cossi, M.; Cammi, R.; Mennucci, B.; Pomelli, C.; Adamo, C.; Clifford, S.; Ochterski, J.; Petersson, G. A.; Ayala, P. Y.; Cui, Q.; Morokuma, K.; Malick, D. K.; Rabuck, A. D.; Raghavachari, K.; Foresman, J. B.; Cioslowski, J.; Ortiz, J. V.; Stefanov, B. B.; Liu, G.; Liashenko, A.; Piskorz, P.; Komaromi, I.; Gomperts, R.; Martin, R. L.; Fox, D. J.; Keith, T.; Al-Laham, M. A.; Peng, C. Y.; Nanayakkara, A.; Gonzalez, C.; Challacombe, M.; Gill, P. M. W.; Johnson, B.; Chen, W.; Wong, M. W.; Andres, J. L.; Head-Gordon, M.; Replogle, E. S.; Pople, J. A. *Gaussian 98*, Revision A.6; Gaussian, Inc.: Pittsburgh, PA, 1998.

(37) (a) Becke, A. D. *Phys. Rev*. **1988**, *A38*, 3098. (b) Lee, C.; Yang, W.; Parr, R. G. *Phys. Rev*. **1988**, *B37*, 785. (c) Becke, A. D. *J. Chem. Phys*. **1993**, *98*, 5648.

(38) (a) Ditchfield, R. *Mol. Phys*. **1974**, *27*, 789. (b) Wolinski, K.; Hilton, J. F.; Pulay, P. *J. Am. Chem. Soc*. **1990**, *112*, 8257.

(39) Wasylishen, R. E.; Mooibroek, S.; Macdonald, J. B. *J. Chem. Phys*. **1984**, *81*, 1057.

(40) (a) Christ, H. A.; Diehl, P.; Schnieder, H. R.; Dahn, H. *Helv. Chim. Acta* **1961**, *44*, 865. (b) Figgis, B. N.; Kidd, R. G.; Nyholm, R. S. *J. Chem. Soc*. **1962**, 469. (c) Burgar, M. I.; St. Amour, T. E.; Fiat, D. *J. Phys. Chem*. **1981**, *85*, 502.

(41) Brown, R. D.; Godfrey, P. D.; Storey, J. *J. Mol. Spectrosc*. **1975**, *58*, 445.

(42) Godfrey, P. D.; Brown, R. D.; Hunter, A. N. *J. Mol. Struct*. **1997**, *413/414*, 405.

(43) Rousseau, B.; Van Alsenoy, C.; Keuleers, R.; Desseyn, H. O. *J. Phys. Chem. A* **1998**, *102*, 6540.

(44) Eggenberger, R.; Gerber, S.; Huber, H.; Searles, D.; Welker, M. *J. Mol. Spectrosc*. **1992**, *151*, 474.

(45) (a) Ludwig, R.; Weinhold, F.; Farrar, T. C. *J. Chem. Phys*. **1995**, *103*, 6941. (b) *J. Chem. Phys*. **1996**, *105*, 8223.

(46) De Luca, G.; Russo, N.; Köster, A. M.; Calaminici, P.; Jug, K. *Mol. Phys*. **1999**, *97*, 347.

(47) Bailey, W. C. *Chem. Phys. Lett.* **1999**, *292*, 71.

(48) Pyykkö, P. *Z. Naturforsch*. **1992**, *47a*, 189.

(49) Frerking, M. A.; Langer, W. D. *J. Chem. Phys*. **1981**, *74*, 6990.

(50) Cornet, R.; Landsberg, B. M.; Winnewisser, G. *J. Mol. Spectrosc*. **1980**, *82*, 253.

(51) (a) Verhoeven, J.; Dymanus, A.; Bluyssen, H. *J. Chem. Phys*. **1969**, *50*, 3330. (b) Bellet, J.; Lafferty, W. J.; Steenbeckeliers, G. *J. Mol. Spectrosc*. **1973**, *47*, 388. (c) De Lucta, F. C.; Helminger, P. *J. Mol. Spectrosc*. **1975**, *56*, 138.

(52) Palmer, M. H. *Z. Naturforsch*. **1996**, *51A*, 442.

(53) Merke, I.; Dreizler, H. *Z. Naturforsch*. **1987**, *42A*, 1043.

(54) Wasylishen, R. E.; Macdonald, J. B.; Friedrich, J. O. *Can. J. Chem*. **1984**, *62*, 1181.

(55) (a) Chesnut, D. B.; Phung, C. G. In *Nuclear Magnetic Shieldings and Molecular Structure*; Tossell, J. A., Ed.; Kluwer Academic Publishers: Dordrecht, The Netherlands, 1993; p.221. (b) Chesnut, D. B. *Annu. Rep. NMR Spectrosc*. **1994**, *29*, 71.

(56) Kutzelnigg, W.; Fleischer, U.; Schindler, M. In *NMR−Basic Principles and Progress*; Springer-Verlag: Berlin, 1990; Vol. 23, p 165.

(57) Chesnut, D. B.; Phung, C. G. *J. Chem. Phys*. **1989**, *91*, 6238.

(58) Kaupp, M.; Malkin, V. G.; Malkina, O. L.; Salahub, D. R. *J. Am. Chem. Soc*. **1995**, *117*, 1851.

(59) (a) Schreckenbach, G.; Ziegler, T. *J. Phys. Chem*. **1995**, *99*, 606. (b) Ruiz-Morales, Y.; Schreckenbach, G.; Ziegler, T. *J. Phys. Chem*. **1996**, *100*, 3359.

(60) (a) Gauss, J. *Chem. Phys. Lett*. **1992**, *191*, 614. (b) Gauss, J.; Stanton, J. F. *J. Chem. Phys*. **1996**, *104*, 2574.

(61) Hansen, P. E.; Abildgaard, J.; Hansen, A. E. *Chem. Phys. Lett*. **1994**, *224*, 275.

(62) Barszczewicz, A.; Jaszunski, M.; Jackowski, K. *Chem. Phys. Lett*. **1993**, *203*, 404.

(63) Olah, G. A.; Burrichter, A.; Rasul, G.; Gnann, R.; Christe, K. O.; Prakash, G. K. S. *J. Am. Chem. Soc*. **1997**, *119*, 8035.

(64) Kaupp, M.; Malkina, O. L.; Malkin, V. G. *J. Chem. Phys*. **1997**, *106*, 9201.

(65) (a) Butler, L. G.; Cheng, C. P.; Brown, T. L. *J. Am. Chem. Soc*. **1981**, *103*, 2738. (b) Butler, L. G.; Brown, T. L. *J. Am. Chem. Soc*. **1981**, *103*, 6541.

(66) Gready, J. E. *J. Phys. Chem*. **1984**, *88*, 3497.

(67) Malkin, V. G.; Malkina, O. L.; Salahub, D. R. *J. Am. Chem. Soc*. **1995**, *117*, 3294.

(68) Gao, Q.; Jeffrey, G. A.; Ruble, J. R.; McMullan, R. K. *Acta Crystallogr*. **1991**, *B47*, 742.
(69) Kallies, B.; Kleinpeter, E.; Koch, A.; Mitzner, R. *J. Mol. Struct*. **1997**, *435*, 123.
(70) Cheng, C. P.; Brown, T. L. *J. Am. Chem. Soc*. **1979**, *101*, 2327.
(71) Ramsey, N. F. *Phys. Rev*. **1950**, *78*, 699.
(72) *72. Handbook of Data on Organic Compounds*; Lide, D. R., Milne, G. W. A., Eds.; CRC Press: Boca Raton, FL.; 1994; Vol. I.
(73) Elbert, S. T.; Davidson, E. R. *Int. J. Quan. Chem*. **1974**, *8*, 857.
(74) Ditchfield, R.; Del Bene, J. E.; Pople, J. A. *J. Am. Chem. Soc*. **1972**, *94*, 703.
(75) Jameson, C. J.; Gutowsky, H. S. *J. Chem. Phys*. **1964**, *40*, 1714.
(76) Gierke, T. D.; Flygare, W. H. *J. Am. Chem. Soc*. **1972**, *94*, 7277.
(77) Scheubel, W.; Zimmermann, H.; Haeberlen, U. *J. Magn. Reson*. **1985**, *63*, 544.
(78) Contreras, R. H.; Biekofsky, R. R.; Esteban, A. L.; Diez, E.; Fabian, J. S. *Magn. Reson. Chem*. **1996**, *34*, 447.